Welded fuses for dissipative beam-to-column connections of composite steel frames: Numerical analyses

Marco Valente *, Carlo A. Castiglioni, Alper Kanyilmaz

Department of Architecture, Built Environment & Construction Engineering ABC, Politecnico di Milano, Piazza Leonardo da Vinci 32, 20133 Milan, Italy

An innovative repairable fuse device for moment-resisting composite steel frames is numerically investigated in this study developed within the European research project "Fuseis". The fuse device consists of steel plates welded to the web and bottom flange of the beam with a specifically detailed gap in the concrete slab. In case of damage after a severe seismic event, the repair work is limited only to the replacement of the fuse. The results of preliminary numerical analyses carried out on detailed finite element models of beam-to-column sub-assemblages show that the dissipative fuses are able to concentrate plastic deformations in the steel plates protecting the other structural elements. Parametric investigations are performed to examine the influence of some relevant geometric characteristics of the flange plate on the fuse behavior. Then, a simplified numerical model of the device is developed and calibrated using the results of experimental tests carried out on beam-to-column sub-assemblages. The effects of the application of the device on the seismic performance of multi-storey composite steel frames are investigated through non-linear dynamic and static analyses. The results of the numerical anal-yses show the effectiveness of the fuse devices to dissipate large amounts of plastic energy and to preserve the other structural elements from damage. The influence of both the main mechanical characteristics and different locations of the fuses is also discussed in terms of relative seismic performance of the composite steel frames under study.

Keywords:
Welded fuse devices
Energy dissipation
Numerical analyses
Seismic performance
Composite steel frames

Article history:
Received 29 March 2016
Received in revised form 30 August 2016
Accepted 14 September 2016
Available online 30 September 2016

1. Introduction

Under strong earthquakes building structures may experience severe damage in the main structural elements that are not easily repairable. A simple and cost-effective repair of the damaged parts of the structures is a critical issue for seismic strengthening of structures and still represents an interesting research subject in earthquake-resistant design. According to the provisions of modern seismic codes, in moment-resisting frames beams are the dissipative zones and damage may occur at the beam ends near the beam-to-column connections. Failures of beam-to-column connections of steel buildings in past earthquakes generated concern about the reliability and high repair costs of conventional steel moment connections. Different alternative methods have been suggested for improving the seismic behavior of connections, moving the likely plastic hinges in beams away from the column face [1]. A ductile fuse can be created to accommodate the plastic deformation that is required for seismic energy dissipation while protecting the beam-to-column joints. Structural systems that may be easily and economically repairable are considered as effective and attractive in high seismicity regions due to the reduction of possible repair costs.

* Corresponding author.
E-mail address: marco.valente@polimi.it (M. Valente).

The work described in this paper is developed within a European research program named "Fuseis" [2–5]. The aim of the "Fuseis" project is to develop innovative fuse devices for moment-resisting composite steel frames, with the following functional objectives: 1) inelastic deformations are concentrated in the devices that act as dissipative fuses; 2) the fuses can be easily fabricated, installed and removed, limiting repair costs and time required to make the structure operational after severe earthquakes. A simplified scheme of the fuse device placed in a moment-resisting composite steel frame is sketched in Fig. 1. The innovative system is a moment-resisting frame in which the beams are cut near their ends and continuity is provided by means of additional steel plates (fuse devices) that are welded to the web and the lower flange of the beams. Potential plastic hinges are supposed to take place in the middle of the fuse device away from the connection. In conventional moment-resisting frames beams generally have large and heavy sections, carry gravity loads and are difficult to be replaced. In innovative seismic-resistant steel frames with dissipative fuses, repair work, if needed, is limited only to the replacement of the additional steel plates.

Within the "Fuseis" research project, experimental investigations on the welded fuse behavior under cyclic loading were performed at Instituto Superior Tècnico of Lisbon and detailed results are extensively reported in [2]. The work described in this paper presents the numerical

Published Journal Article available at: http://dx.doi.org/10.1016/j.jcsr.2016.09.003

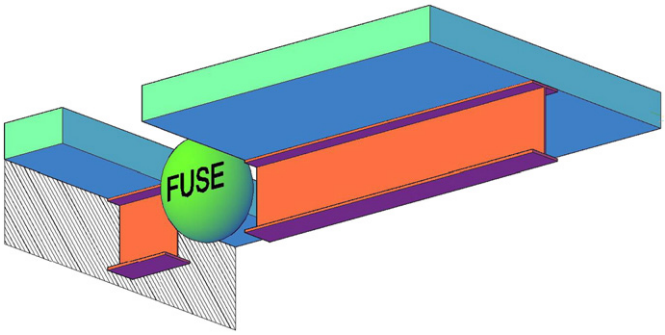

Fig. 1. Schematic representation of a fuse device placed in a moment-resisting composite steel frame.

investigations carried out in support of the experimental campaign in order to study the cyclic behavior of the welded fuse devices. Then, numerical analyses are performed to assess the effects of the application of welded fuse devices on the seismic performance of multi-storey composite steel frames.

The fuse device behavior is studied by means of two different numerical approaches. First, the refined three-dimensional finite element modeling technique, for which the computational effort is very expensive, is employed. Detailed finite element models using solid elements are developed to have a better understanding of the behavior of the fuse system and to demonstrate that the whole plasticization occurs only in the device. Then, a lumped plasticity modeling approach is employed and global numerical models are created through a computer code commonly used by structural engineers in order to analyze the seismic response of different multi-storey composite steel frames equipped with fuse devices. Special non-linear link elements are used to simulate the non-linear behavior of the fuse derived from the results of experimental tests. After the calibration of the models according to the test results, non-linear dynamic and static pushover analyses are carried out to assess and compare the effectiveness of the fuse devices with different geometric and mechanical characteristics.

2. Preliminary numerical analyses of detailed finite element models

An extensive preliminary numerical study was carried out before the execution of the experimental tests of the "Fuseis" research project. The aims of these introductory numerical analyses were: 1) to define the main geometric and mechanical properties of both the devices and the specimens to be experimentally tested; 2) to identify the optimal configurations for the welded fuse solution studying the influence of the most relevant variables; 3) to anticipate the overall behavior of the test specimens with fuse devices. A three-dimensional finite element idealization allows for the representation of the local details of the members geometry and its use is essential to detect stress concentrations and local damage patterns, [6–8]. This preliminary numerical study provided useful information about the dimensions of both the fuse system and the experimental specimens.

2.1. Finite element models

Detailed three-dimensional finite element models were developed through the computer code Abaqus [9] in order to reproduce the behavior of the fuse device under monotonic and cyclic loading and to perform parametric analyses. First, an introductory three-dimensional finite element model of a steel beam with composite slab was created to identify the mechanical and geometric parameters influencing the cyclic performance of the fuse device, Fig. 2. Then, more refined three-dimensional finite element models of a composite beam connected to a column were developed to anticipate the behavior of the specimens tested at Instituto Superior Tècnico of Lisbon, Fig. 2. The different flange plates of the fuse device used in the experimental tests were modeled and represented in Fig. 3. Finally, a three-dimensional finite element model of a portion of a storey of a composite steel frame was used to calibrate and simulate the experimental tests performed at Politecnico di Milano, Fig. 4.

The elements used in the different models are all chosen from those available in ABAQUS/Standard library. All steel parts and concrete slab were modeled using the solid (continuum) elements named C3D8R. These elements are linear displacement interpolation solid elements with reduced integration. Reduced integration elements are chosen in order to reduce computational time, which would be excessive in the case of higher order elements. The mesh is finer in the parts of the model where high stress concentrations are expected. The steel plates of the fuse device are tied to the web and bottom flange of the beam through the weld parts. Shear connection between slab and beam and all other constraints are modeled by using the "tie" option. Using such a constraint type, the degrees of freedom (rotational and translational) between the nodes of the two surfaces that are "tied" to each other are constrained to maintain the same values.

Structural steel and reinforcing rebars in the slab are assumed to behave like an elastic-plastic material with hardening both in compression and in tension and the Von Mises yield criterion is adopted. The steel grades S275 and A500 are used, respectively, for structural elements and reinforcing rebars of the finite element model representing the test specimens.

Numerical analyses and experimental tests showed that the behavior of the fuse was mainly dependent on the yielding and buckling of the steel plates and no major cracking of the slab was observed. Consequently, in preliminary numerical models concrete was modeled with an elastic behavior, thus reducing the high computational demand. Buckling of the flange plate was properly simulated at hogging rotation.

In this study the finite element models were analyzed in terms of deformed shape and equivalent plastic strain (PEEQ) contour plot. The equivalent plastic strain PEEQ is defined as $\mathrm{PEEQ} = \sqrt{\frac{2}{3}\varepsilon_{ij}^{p}\varepsilon_{ij}^{p}}$ and it

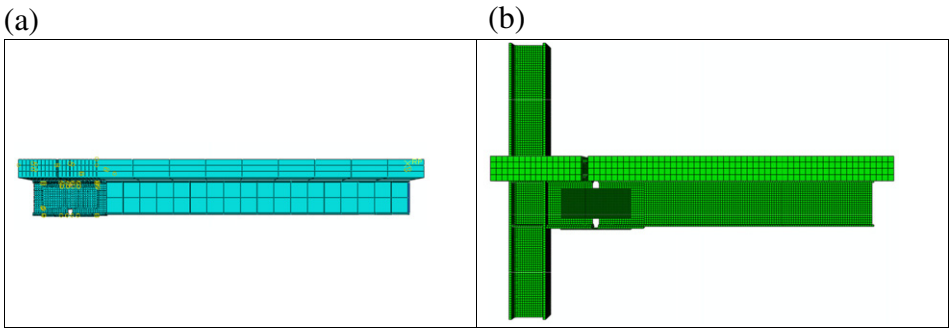

Fig. 2. (a) Preliminary finite element model of a composite steel beam with fuse device; (b) Final proposal of the configuration of a beam-to-column sub-assemblage with fuse device.

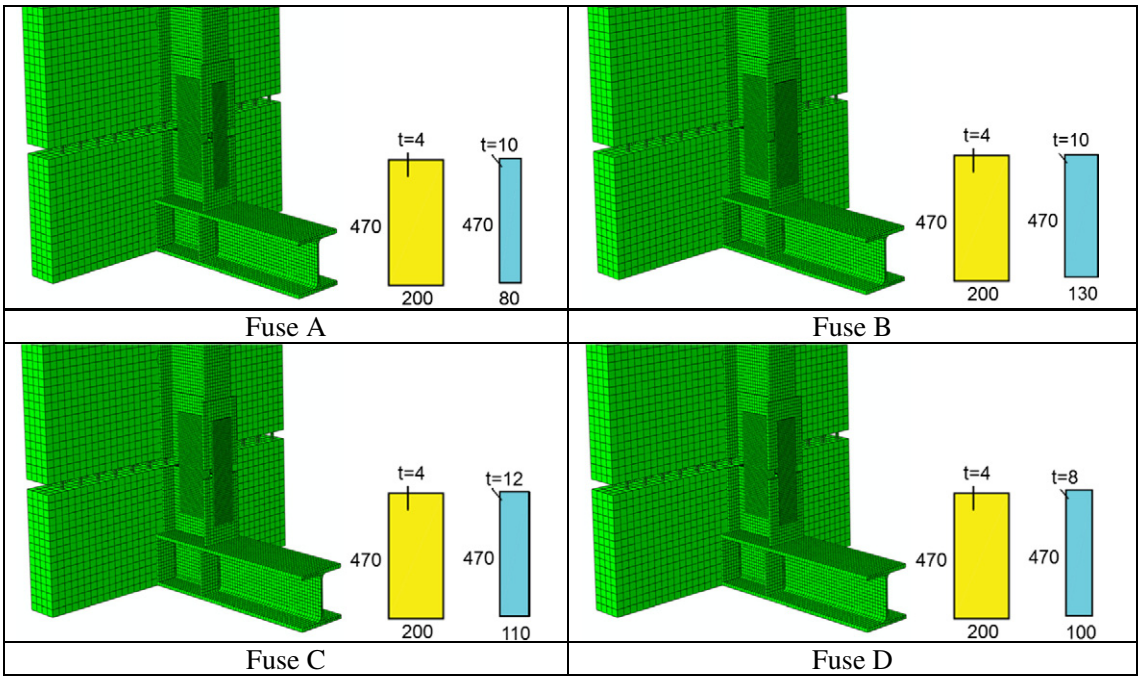

Fig. 3. Finite element models of the specimens used for experimental tests: dimensions of the web (yellow) and flange (blue) plates (dimensions in mm).

represents the equivalent plastic strain accumulated during the displacement-controlled loading history.

2.2. Preliminary parametric investigations of the fuse device

The initial simplified finite element model consisted of a composite steel beam with an IPE240 section profile supporting a 150 mm thick reinforced concrete slab. A welded fuse device was inserted in the beam and a specifically detailed gap was created in the concrete slab in order to allow for large plastic rotations in the fuse without causing crushing in the concrete slab. Steel rebars were continuous over the gap and were designed in order to force the plastic neutral axis to lie within the slab thickness. A displacement-controlled cycling loading history was applied at the beam edge and the cyclic response of the fuse device was numerically investigated. The results obtained from the simplified numerical models were qualitatively analyzed and compared under sagging and hogging bending for different joint rotations. Parametric analyses were performed to identify the influence of some geometric and mechanical variables and to define effective configurations for the fuse device. In particular, the cyclic behavior of the fuse was analyzed changing selected geometric and mechanical parameters, such as the geometric slenderness and the resistance capacity ratio.

The geometric slenderness λ of the flange plate is defined as:

$$\lambda = \frac{L_0}{t_{fuse}} \tag{1}$$

where L_0 is the free buckling length of the fuse and t_{fuse} is the thickness of the flange plate. The free buckling length L_0 is given by the horizontal distance between the edges of the lap welds on each side of the gap on the fuse section.

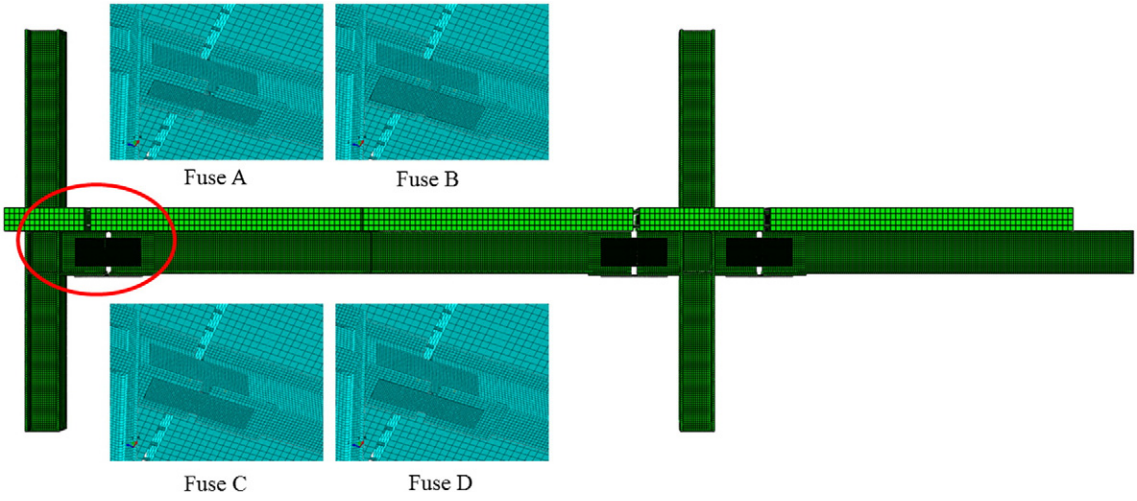

Fig. 4. Finite element model of a portion of a storey of a composite steel frame with different fuse devices.

Table 1
Main dimensions and geometric slenderness λ of the welded flange plates of the fuses.

Flange plate	A	B	C	D
Thickness [mm]	10	10	12	8
Width [mm]	80	130	110	100
Cross-section area [mm^2]	800	1300	1320	800
Geometric slenderness	17	17	14.1	21.25

The resistance capacity ratio α of the fuse is defined as:

$$\alpha = \frac{M_{max,fuse}}{M_{pl,beam}} \quad (2)$$

where $M_{max,fuse}$ is the maximum moment developed by the fuse device and $M_{pl,beam}$ is the plastic resisting moment of the unreinforced area of the composite beam cross-section.

The finite element model was subjected to imposed cyclic displacements applied at the beam edge and the overall behavior of the joints was summarized by means of moment-rotation diagrams in order to represent the hysteretic response. The cyclic behavior of the joints was overall stable and ductile; the strength loss under hogging bending was caused by the buckling of the lower flange plate. The effects of the variation of the plate thickness, the free buckling length and the plate section were investigated by performing parametric analyses. For the sake of conciseness, in this paper only a qualitative description of the main results of these preliminary parametric analyses is reported.

The first series of analysis was performed on numerical models with the same free buckling length ($L_0 = 150$ mm) of the welded plates and the flange plate thickness was assumed as the variable parameter. The increase of the thickness was obtained maintaining the same cross-section area of the plate by changing the plate width. The increase of the moment of inertia of the plates causes an enlargement of the cycle and an enhancement of the plastic energy dissipated by the model.

The second series of analysis was carried out on numerical models with the same thickness of the plates and the free buckling length of the welded plates was assumed as the variable parameter. An increase of the free buckling length causes both the loss of stiffness and the decrease of the plastic energy dissipated by the model. Clearly, a reduction of the distance between the edges of the welds decreases the possibility of the flange plate buckling.

The third series of analysis was conducted on numerical models with different plate cross-sections obtained by means of an increase of the plate thickness. An enlargement of the cross-section of the flange plate causes an increase of both the moment capacity and the energy dissipation of the fuse. However, large increases of the flange plate cross-section are not suggested because they may alter the strength hierarchy that prevents concentration of plastic deformation in the irreplaceable parts of the beam: in this case, the aim of the project is not achieved because the whole plastic deformation is not concentrated only in the fuse.

The preliminary analyses of the simplified numerical models proved the effectiveness of the fuse devices, highlighted the influence of some geometric and mechanical parameters, and concluded with the definition of a suitable final configuration for the fuse device, see Fig. 2. A comprehensive description of the results of the preliminary numerical parametric investigations is reported in [10].

2.3. Numerical simulations of the beam-to-column sub-assemblage model

The results of the preliminary analyses of the simplified finite element models of the composite steel beam were used to define different suitable configurations of the fuse devices for the specimens of the laboratory tests. This section presents the results of the numerical simulations of the detailed finite element models representing the specimens of the experimental tests. The different parts of the models were carefully created to match the same dimensions of the test specimens. The finite element model was a typical beam-to-column sub-assemblage, comprising a HEB 240 steel column and a composite beam with an IPE300 section profile supporting a 150 mm thick and 1450 mm wide reinforced concrete slab. The fuse device consisted of steel plates welded to the web and bottom flange of the beam with a specifically detailed gap in the concrete slab. The longitudinal steel rebars of the concrete slab were continuous over the gap in order to ensure transmission of stresses. To assess the performance of the devices, monotonic and cyclic analyses were carried out on the models equipped with fuses with different geometric properties. The same web plate was used for the fuse device in all the models, while the geometric dimensions

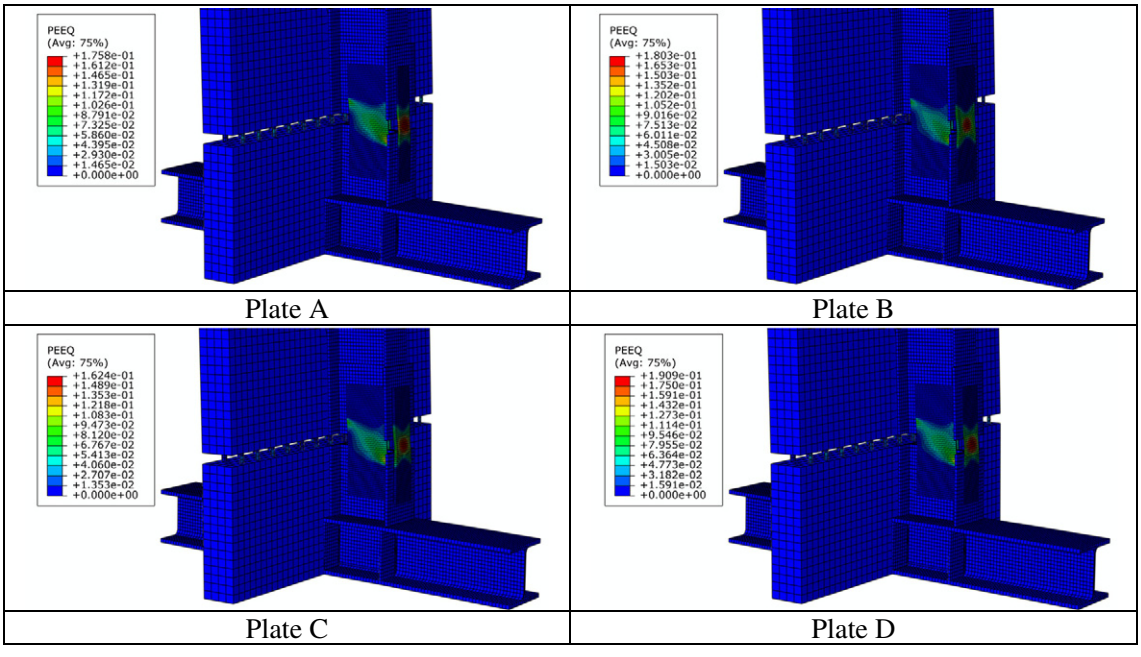

Fig. 5. PEEQ contour plot for the models with different flange plates under sagging rotation (imposed top displacement = 80 mm).

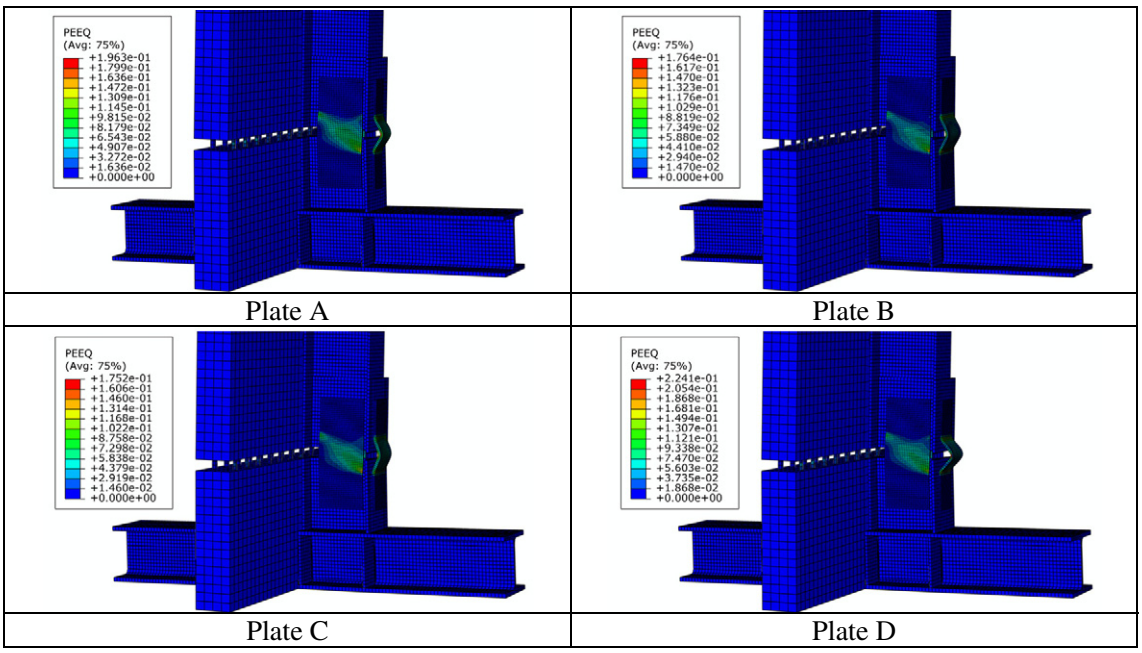

Fig. 6. PEEQ contour plot for the models with different flange plates under hogging rotation (imposed top displacement = 80 mm).

(thickness and width) of the flange plates were different. The same free buckling length, equal to 170 mm, was initially assumed for all the configurations of the fuses. Table 1 summarizes the dimensions (thickness and width) and the geometric slenderness of the welded flange plates of the fuses investigated in the numerical analyses.

The results obtained from the numerical simulations carried out through a displacement-controlled increasing (monotonic) loading history applied at the top edge of the beam are reported in this study.

Fig. 5 shows the deformed shape and the PEEQ contour plot for the models with different plates under sagging rotations (imposed top displacement = 80 mm). In all the models plastic deformations concentrate in the web and flange plates, ensuring that the plastic hinge occurs at the fuse section and protecting the remaining parts of the joint. High values of PEEQ and stress concentrations are registered near the welds of the web plates and in the middle of the flange plates. Typical failure modes observed in the specimens tested in laboratory consisted of the development of cracks at the mid-section of the flange plate under tension. The models with the weakest flange plates exhibit the highest values of PEEQ in the fuse devices.

Fig. 6 presents the deformed shape and the PEEQ contour plot of the fuse device under hogging rotation (imposed top displacement = 80 mm) for the different models. The results of the analyses indicate that both the column and the composite beam remain in the elastic range for all the different plates. The pronounced curved shapes of the plates indicate that the attempt of modeling the buckling behavior of the plates is achieved successfully. It is apparent that strength in the hogging configuration is controlled by buckling, which occurs as a function of both the geometric properties of the flange plates and the free buckling length of the fuse. Numerical results show that the hogging resistance of the fuse is more sensitive to a geometry variation of the flange plates than the sagging resistance. Buckling of the flange plate of the fuse is clearly observed for the models with plates A and D, while in the models with plates C and B buckling of the flange plate under hogging rotations is less evident.

When sagging and hogging behavior is compared, a more significant loss of stiffness occurs under hogging rotation due to buckling of the fuse plate. The severity of yielding and buckling of the plates has a fundamental influence on the performance of the fuse device.

The effects of different free buckling lengths were also investigated in the beam-to-column sub-assemblage models. Fig. 7 shows the PEEQ contour plot at sagging (left) and hogging (right) rotations (imposed top displacement = 80 mm) for the model with flange plate A and free buckling length equal to 140 mm. Comparing the results with the model with the same plate and free buckling length equal to 170 mm, it can be noted that buckling of the flange plate is less evident, plastic deformations are concentrated in a smaller region of the plates and higher values of PEEQ are registered in the fuse device.

Fig. 8 presents the PEEQ contour plots in the models with plates B and D under sagging and hogging rotations at the onset of plastic deformations. In all the models the plastic deformations involve the flange

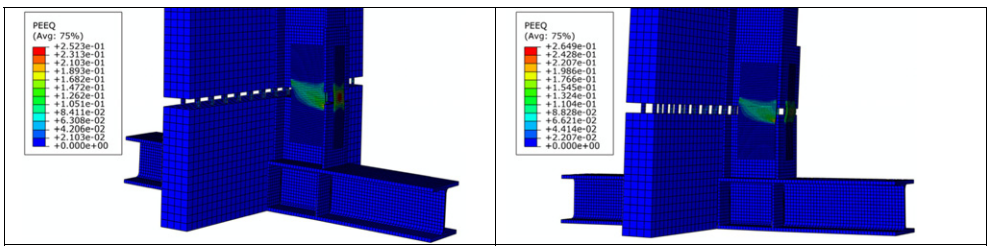

Fig. 7. PEEQ contour plot for the model with plate A and free buckling length equal to 140 mm under both sagging (left) and hogging (right) rotations (imposed top displacement = 80 mm).

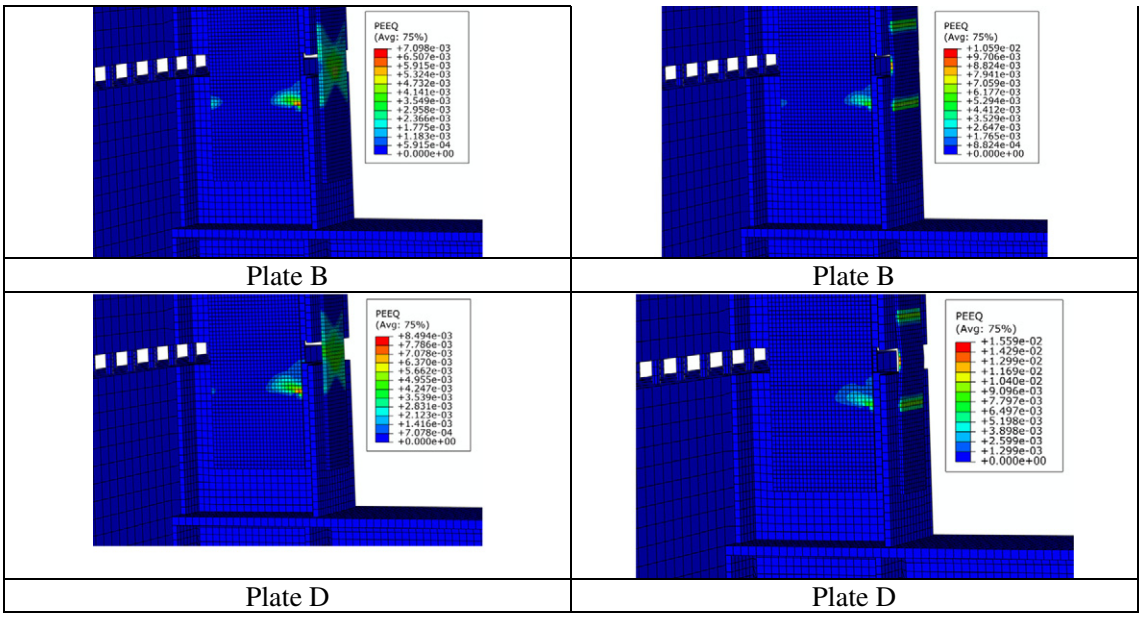

Fig. 8. PEEQ contour plot for the models with plates B and D under both sagging (left) and hogging (right) rotations at the onset of plastic deformations.

plates and the bottom part of the web plate. In the case of sagging rotations, uniform distributions of plastic deformation are observed in the flange plate. In the case of hogging rotations, plastic deformations concentrate near the end of the weld and in the central part of the flange plate.

2.4. Numerical simulations of the frame sub-assemblage model

The finite element model of the fuse was then inserted in a portion of a storey of a composite steel frame in order to anticipate the behavior of the specimen tested at Politecnico di Milano. The frame consisted of two HEB240 steel columns, two IPE300 steel beams and a 150 mm thick reinforced concrete slab, Fig. 4. Welded fuse devices were included in this preliminary numerical model of the frame sub-assemblage, though the experimental tests were carried out with bolted plates. In the finite element model the columns bottom edges were restrained with hinges and displacements were imposed at the columns top edges. Fig. 9 shows both the deformed shape of the numerical model of the frame sub-assemblage and the PEEQ contour plot near the beam-to-column connections. The results obtained with the frame model confirm the outcomes observed in the beam-to-column sub-assemblage models. The objectives of the "Fuseis" research project were achieved because all the potential damage was concentrated only in the fuses. In fact, plastic deformations were registered only in the device regions, while both the columns and the composite beams remained in the elastic range. Buckling of the flange plate can be observed in the internal beam-to-column connection under hogging rotation.

3. Experimental tests and calibration of simple models of the fuse device

3.1. Experimental tests

After the preliminary numerical analyses carried out with refined finite element models, within the "Fuseis" research project, laboratory tests were performed on beam-to-column sub-assemblages at Instituto

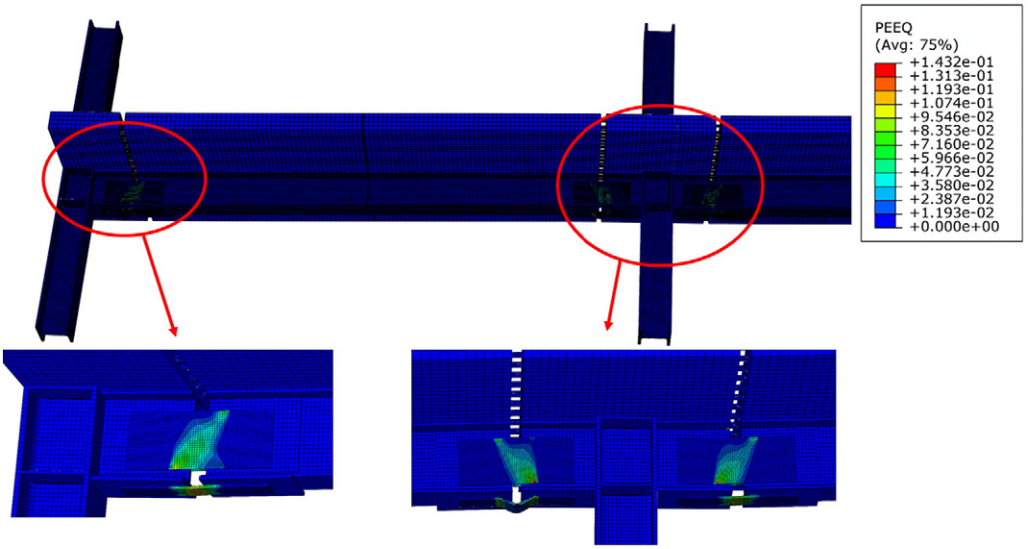

Fig. 9. Deformed shape and PEEQ contour plot in the frame sub-assemblage model (imposed top displacement = 80 mm).

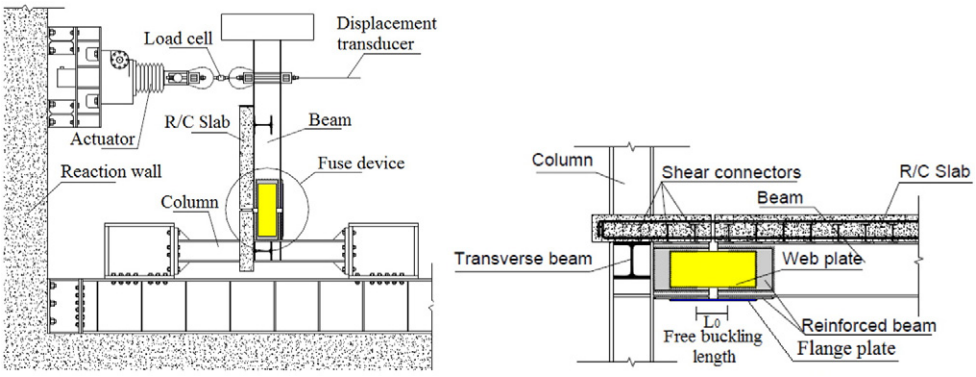

Fig. 10. Experimental test set-up and fuse device configuration.

Superior Tècnico of Lisbon in order to characterize the experimental behavior of the welded fuse devices. Fig. 10 shows the experimental test set-up, the specimen and the fuse device configuration. The dimensions and the geometric slenderness of the welded flange plates of some fuses investigated in the experimental tests are reported in Table 1. The beam-to-column sub-assemblages equipped with welded flange plates E and F were the last specimens to be tested during the experimental campaign and they have not been considered in this study for the calibration of the numerical models because the experimental results obtained from these plates were significantly affected by the effects of accumulated damage induced by previous tests.

The laboratory tests were conducted by applying cyclic variable amplitude displacements at the top of the beam of the specimens. The experimental tests confirmed the main results obtained through the preliminary numerical analyses on detailed finite element models. The proposed devices were able to concentrate plastic deformations in the steel plates and to dissipate large amounts of plastic energy through stable cyclic behavior. The failure modes of the cyclically tested specimens consisted of the development of cracks at the mid-section of the flange plate under tension, whereas both the column and the composite beam remained in the elastic range. The devices could be replaced by unwelding the damaged plates and welding the new ones. A comprehensive description of the results of the extensive experimental campaign can be found in [2].

3.2. Development and calibration of simple numerical models

Simplified numerical models of the beam-to-column sub-assemblages tested at Instituto Superior Tècnico of Lisbon were developed by using the computer code SAP2000 [11]. The numerical models were later used to further investigate the effects of the application of the fuse devices on the seismic response of different multi-storey composite steel frames. The models consisted of a composite steel beam, equipped with fuse devices, connected to a column with the same geometry used in the experimental test set-up. The potential non-linear behavior of the beam was simulated with a lumped plasticity approach by defining a non-linear plastic hinge at the beam end connected to the column. The fuses were modeled as non-linear link elements with a length equal to the free buckling length of the device. The link element is a non-linear spring with six independent internal deformations for which a non-linear generalized force-deformation relationship can be defined. The multi-linear plastic pivot model was used as hysteresis

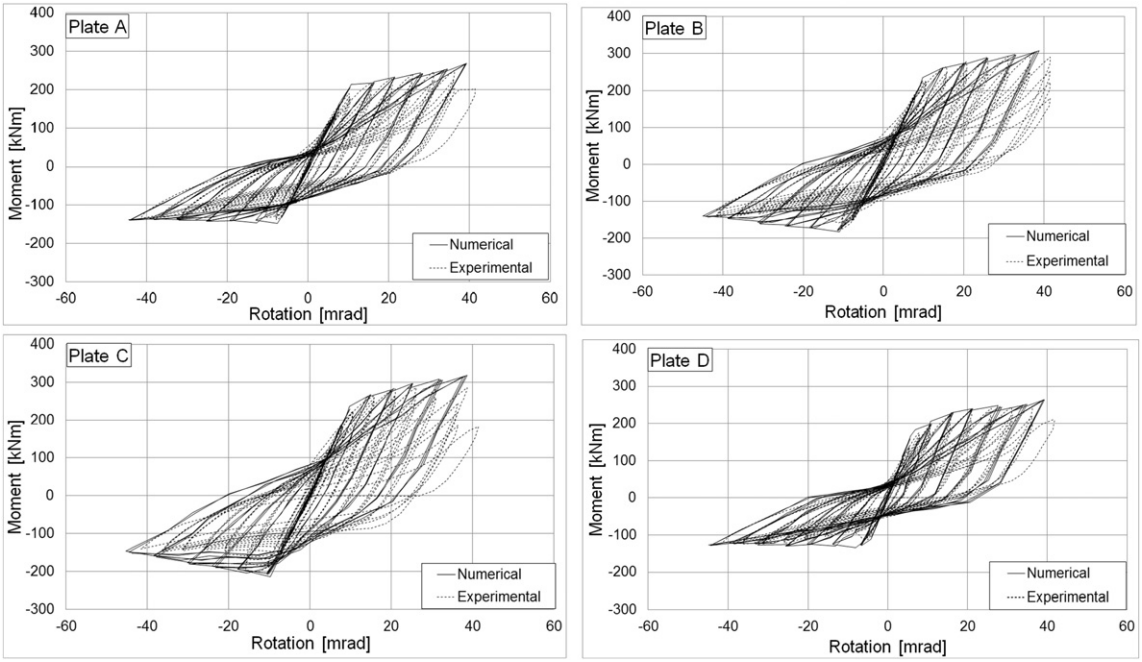

Fig. 11. Comparison of experimental and numerical moment-rotation diagrams of the welded fuses tested at Instituto Superior Tècnico of Lisbon and investigated in this study.

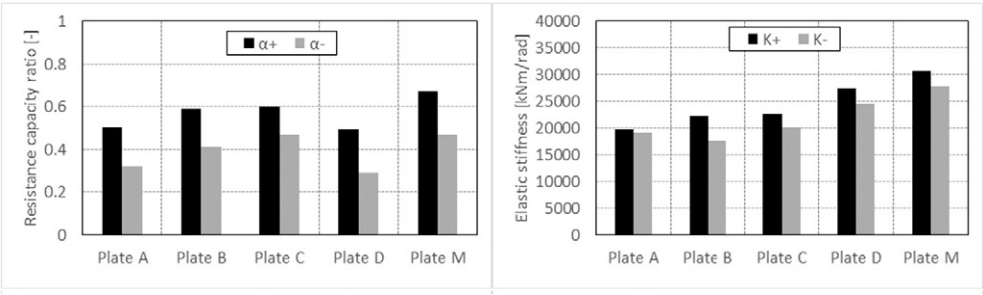

Fig. 12. Resistance capacity ratio (left) and elastic stiffness (right) for sagging and hogging rotations for the welded fuses with different flange plates.

rule including asymmetrical cross-section behavior with pinching and strength degradation. The link behavior was defined by a moment-rotation curve characterized by positive and negative moment capacities and initial stiffness of the fuse device. The non-linear behavior was assigned only to the rotational degree of freedom of the link with respect to the major axis of inertia. The constitutive law adopted for the non-linear link was able to represent the dissipated energy, the stiffness and the maximum moment of the fuse during the cyclic loading history. The initial input parameters of the monotonic moment-rotation diagram of the fuses were obtained from simplified analytical models described in [2]. The computations of the resistance and stiffness values for all fuses were based on the material properties measured during the experimental campaign. Then, the models were calibrated and refined by using the results of the experimental tests carried out on the specimen sub-assemblages.

The comparison of the experimental and numerical moment-rotation diagrams of the welded fuses is shown in Fig. 11. The models were able to accurately capture the non-linear behavior of the different devices in terms of stiffness, resistance, ductility and dissipated energy. The moment-rotation diagrams show that the hysteretic behavior of the fuses was overall stable and dissipative. It was also characterized by pinching effects on the hysteresis loops of cycling loading due to buckling of the fuse plates under hogging rotation. The buckling of the fuse plate and the presence of the concrete slab explain the asymmetry of the diagram in terms of moments. All fuses were able to achieve rotations at least equal to 35 mrad, which is the minimum value recommended by EN 1998 for structures of high ductility class [12]. The experimental and numerical results clearly show the different behavior between plates with extreme values of the resistance capacity ratio (plates A–D and plates B–C, respectively), mainly due to the pinching phenomenon and to the differences in strength, which directly affect the energy dissipation capacity. A more pronounced stiffness degradation with cycling was registered for devices with lower values of the resistance capacity ratio, especially under sagging rotation. Moreover, flange plates A and D proved to be more sensitive to buckling due to their geometry under hogging rotation, showing more marked pinching effects.

The values of the resistance capacity ratio and elastic stiffness of the welded fuses utilized in this study are reported in Fig. 12, for sagging and hogging rotations. The highest resisting moments were assumed for plates B and C because of the large resistant sections of the plates. Some discrepancies between numerical and experimental values of elastic stiffness were observed for some fuses. In this study it was decided to adopt the values of initial stiffness that more accurately approximate the experimental results for the following analyses on multi-storey composite steel frames.

After the calibration of the numerical models of the welded fuses tested at Instituto Superior Tècnico of Lisbon, another moment-rotation curve, hereafter denoted as plate M, was adopted for the welded fuse devices in this study. The input parameters of the monotonic moment-rotation curve for plate M were obtained from the 3D FE models. Consequently, the initial mechanical characteristics of the fuse were not affected by the deterioration of the specimen sub-assemblage observed during the experimental tests. The numerical moment-rotation diagram assumed for plate M and the monotonic curve derived from the 3D FE model are shown in Fig. 13. The main characteristics (resistance capacity ratio and elastic stiffness) of the numerical model of plate M, along with all the other welded fuses, are reported in Fig. 12. Moreover, Fig. 13 compares the numerical moment-rotation curve of plate M with those of the other plates. It can be noted that plate M presents the highest resistance capacity ratio and elastic stiffness for sagging rotation.

4. Steel frames under study and numerical modeling

Three different multi-storey steel frames with composite beams are analyzed in this study in order to understand the effects of the application of the fuse devices on different types of structures. The seismic response of the frames with and without fuse devices is evaluated and a comparison of the seismic performance of the innovative seismic-resistant steel frames with different fuse plates is carried out too.

The frames under study were extracted from composite steel buildings with different number of storeys. Dead loads consist of the weights of structural components and partitions, and live loads are assumed to

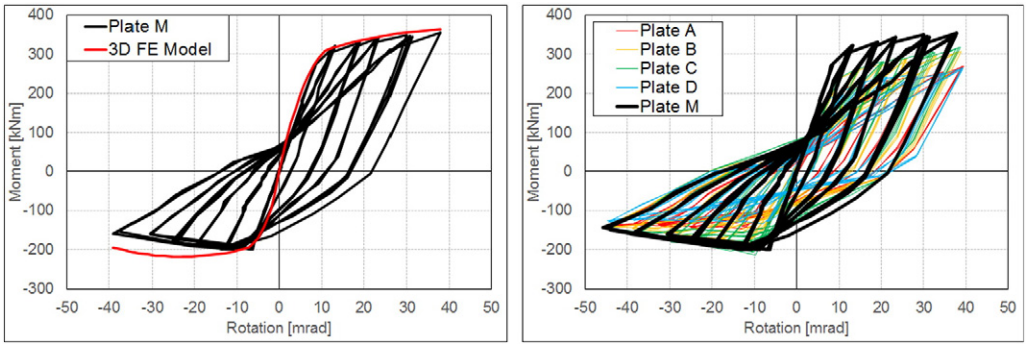

Fig. 13. Numerical moment-rotation diagram for plate M: comparison with the 3D finite element model and with other plates.

be equal to 2 kN/m^2 for all storeys. Storey masses include dead loads and a percentage of live loads (30% according to Eurocode 8 for common residential and office buildings). The steel grade used for all the structural members is S275. The three frames consist of three bays and different number of storeys ranging from three to nine. The storey height and the bay width are equal to 3.5 m and 5 m, respectively. The column section dimensions change as a function of the number of storeys of the frames and range from HE320B for the three-storey frame to HE400B for the nine-storey frame. The composite beams present an IPE300 section profile supporting a 150 mm thick reinforced concrete slab in accordance with the specimen of the experimental test set-up. The geometric dimensions and section profiles of the different frames under study are illustrated in Fig. 14.

Numerical models of both the conventional steel frames without fuse devices and innovative seismic-resistant steel frames with fuse devices were developed using the computer code SAP2000. Hereafter, conventional frames are denoted as "F1 — n" and innovative seismic-resistant frames are denoted as "FPi — n", where n and i indicate the number of the storeys of the frame and the plate type used in the model, respectively.

A lumped plasticity modeling approach was employed for the non-linear models of the frames. Beam and column elements were modeled as frame elements and non-linearity was concentrated in plastic hinges at their ends. To characterize the non-linear behavior of a plastic hinge, the force-displacement properties suggested in FEMA 356 [13] were implemented. Flexural moment hinges were adopted for the beams, while plastic hinges accounting for the interaction between axial force and bending moment were defined for the columns. Beam-to-column joints were considered as rigid in accordance with the connection detailing of the experimental tests.

The models of the different fuse devices were implemented in the numerical models of the frames. The length of the beams was subdivided into different elements in order to take into account both the presence of the fuse devices and the part of the beam reinforced with additional welded plates. The fuses were modeled as non-linear link elements inserted in the beams with a length equal to the free buckling length of the welded plates. The multi-linear plastic pivot model was used as hysteresis rule for the fuses. The values of the parameters used for the hysteretic model were obtained from the calibration of the models of the specimens tested at Instituto Superior Tècnico of Lisbon.

The part of the beam reinforced with additional plates, aimed at avoiding spreading of plasticity into the connection, was reproduced in the numerical models by using different cross-sections and plastic hinges properties around the device. The length of these regions was assumed in the model in accordance with the geometry of the experimental specimens.

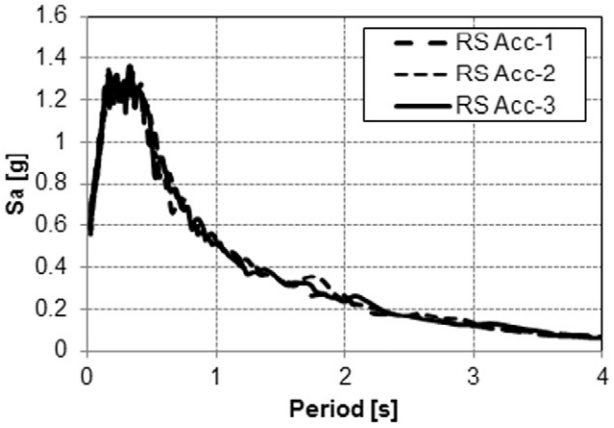

Fig. 15. Response spectra of the artificial accelerograms.

5. Numerical analyses and results

The seismic performance of the frames under study was assessed through non-linear dynamic analyses with response spectrum-compatible artificial accelerograms. The set of artificial ground motions consisted of three different records that were generated so as to match the Eurocode 8 response spectrum (Type 1, soil type A, 5% viscous damping) using the computer code SIMQKE [14]. The response spectra of the artificial accelerograms used in this study are shown in Fig. 15. The non-linear dynamic analyses were performed for three different peak ground accelerations (PGA = 0.3*g*, PGA = 0.5*g* and PGA = 0.7*g*) of the artificial earthquake records. In addition, non-linear static (pushover) analyses were performed in order to assess the distribution of plastic hinges and to check the possible collapse mechanisms.

5.1. Top displacement and base shear

The results of the non-linear dynamic analyses in terms of maximum roof displacement and base shear are presented using the average values obtained through the three artificial records.

The maximum top displacements of the different frames are shown in Fig. 16 for different peak ground accelerations. As can be noted, the maximum top displacements of the innovative frames with fuses are

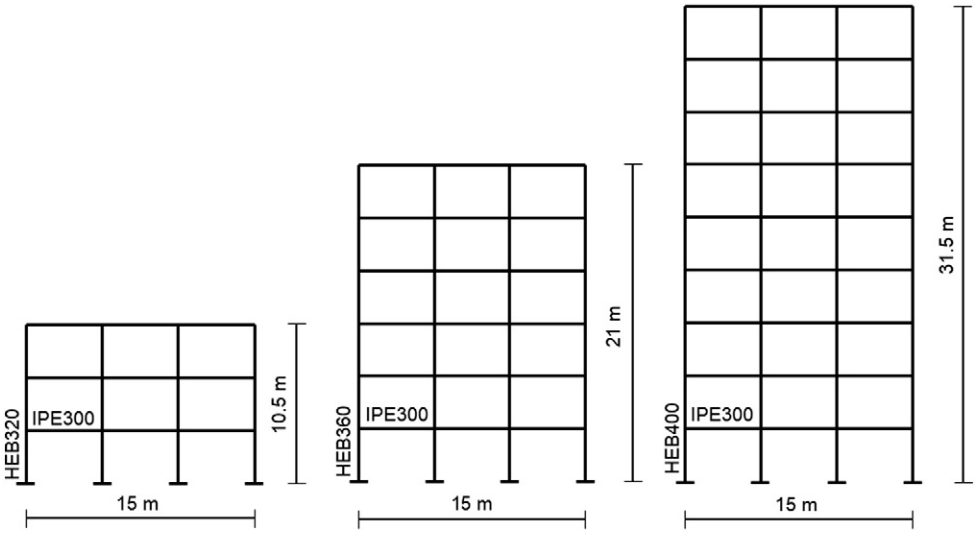

Fig. 14. Steel frames under study.

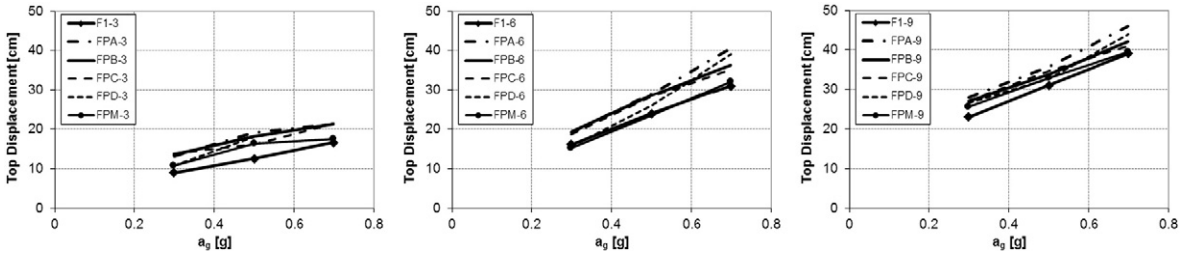

Fig. 16. Maximum top displacement of the frames under study for different peak ground accelerations.

larger than those of the conventional frames because the insertion of the fuse devices has the consequence of reducing the lateral stiffness of the frames.

Comparing the seismic performance of the different innovative frames, it can be argued that the initial stiffness and resisting moments adopted for the constitutive laws of the fuse devices affect the results. In the case of seismic intensity levels equal to PGA = 0.3*g*, frames FPM and FPD generally exhibit smaller top displacements because the moment-rotation curves adopted for the fuse plates M and D present higher elastic stiffness. In the case of seismic intensity levels equal to PGA = 0.7*g*, smaller top displacements are registered for frames FPM, FPB and FPC because the moment-rotation curves adopted for the fuse plates M, B and C present higher resisting moment. In the case of severe ground motions (PGA = 0.7*g*), the conventional frames and the innovative frames FPM show similar values of top displacements for all the different frames. Numerical results highlight that a significant reduction of the mechanical characteristics of the fuse (initial stiffness and resisting moments) can be detrimental to the seismic performance of the innovative frames in terms of top displacements. In particular the innovative frame FPA presents large increases of top displacements for different seismic intensity levels.

Fig. 17 shows the maximum values of the base shear of the frames for different peak ground accelerations. As already explained, the results are reported as average values of the ones obtained through the non-linear dynamic analyses using different accelerograms. The maximum values of the base shear of the innovative frames with fuses are always smaller than those of the conventional frames. The decrease of the base shear of the innovative frames depends mainly on the resistance capacity ratio of the fuse devices. The highest values of the base shear are observed for the frames equipped with fuses with the highest resisting moments (frames FPM, FPB and FPC). The innovative frames FPA and FPD present large decreases of base shear.

5.2. Plastic hinge pattern and energy dissipation

The distribution of plastic hinges is evaluated for conventional and innovative frames at the end of the non-linear dynamic analyses. Fig. 18 compares the plastic hinge patterns in conventional frames F1 and in frames with fuses FPM under Acc-1 with PGA = 0.7*g*. As can be noted, the number and the distribution of plastic hinges are similar for the two types of structures.

In conventional frames plastic deformations occur at the beam ends and at the base of the ground level columns. This result reflects the design of the frames according to the provisions of Eurocode 8. Nevertheless, for high values of peak ground acceleration some plastic hinges are sometimes observed at columns ends too. For instance, the three-storey

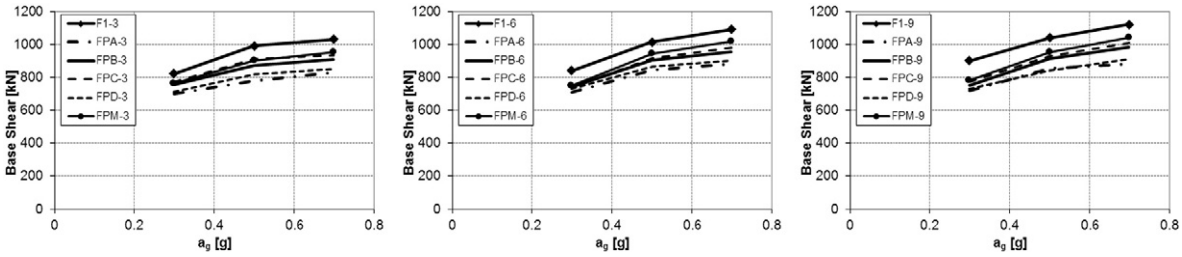

Fig. 17. Maximum base shear of the frames under study for different peak ground accelerations.

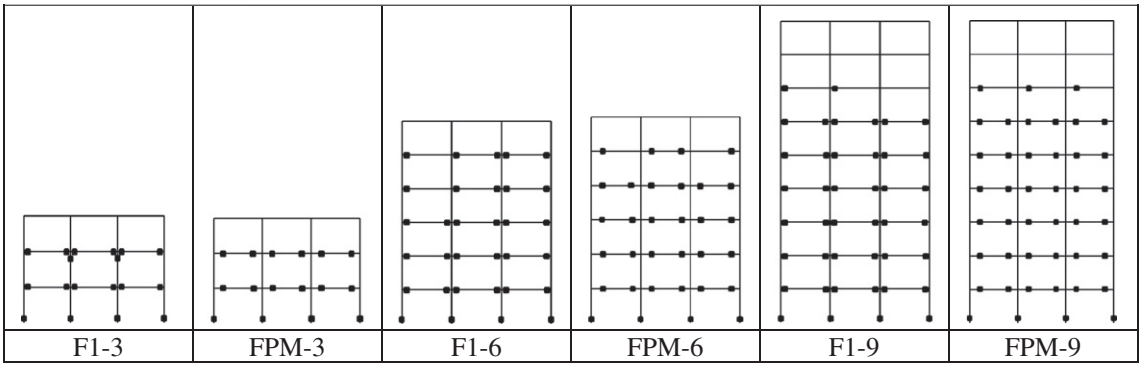

Fig. 18. Plastic hinge patterns in conventional frames (F1) and innovative frames (FPM) under Acc-1 (PGA = 0.7*g*).

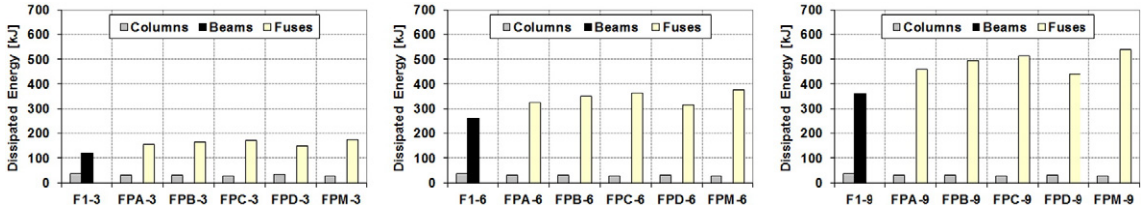

Fig. 19. Plastic energy dissipated in conventional frames (F1) and in innovative frames with fuses (FPA, FPB, FPC, FPD, FPM) under PGA = 0.7*g*.

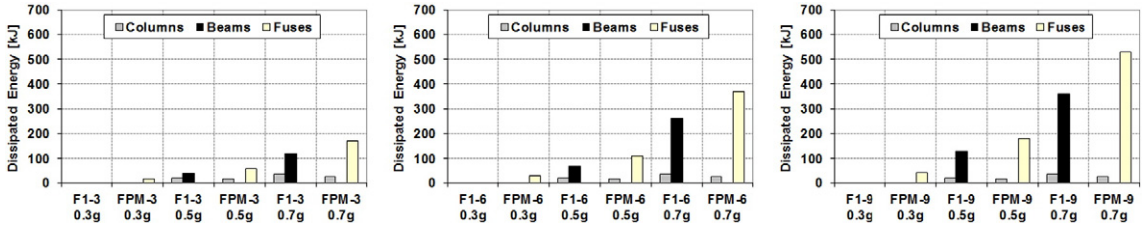

Fig. 20. Plastic energy dissipated in conventional frames (F1) and in innovative frames (FPM) under different peak ground accelerations.

frame F1–3 presents plastic hinges both at the base of the ground level columns and at the second level columns.

Comparing the results with conventional frames, it can be argued that in all cases the application of the fuse devices prevents the formation of plastic hinges in columns, except at the columns base, and the possible activation of a weak-storey collapse mechanism. In innovative frames plastic deformations concentrate only in the fuses and the beam ends are protected remaining in the elastic range. The fuses act as dissipative devices, preventing the spreading of damage into the other structural elements and the pattern of yielding is in perfect agreement with the global mechanism. Finally, numerical results show that no kinematic mechanism is observed for all the frames under study subjected to accelerograms with PGA = 0.7*g*.

Fig. 19 compares the amount of plastic energy dissipated in conventional and innovative seismic-resistant frames with different plates under severe seismic excitation (PGA = 0.7*g*). The plastic energy dissipated in columns, beams and fuses is reported; it is computed as the area enclosed inside all the cycles during the earthquake excitation. As can be noted, the total amount of hysteretic energy dissipated in innovative frames with fuses is higher than in conventional frames. This result can be explained by the higher values of hysteretic energy dissipated by fuses in innovative frames than by beams in conventional frames. The plastic deformation demand and the plastic energy dissipated in columns slightly decrease when fuse devices are present. Moreover, the resistance capacity ratio of the fuses affects the plastic energy dissipated in fuses and columns of innovative frames.

The largest amount of plastic energy is dissipated by frames FPM and FPC for all the different structures. This result confirms the dissipative behavior of these plates shown by the experimental tests. The energy dissipated by frames FPD is smaller than the other innovative frames because of the low energy dissipation capacity of this type of fuse due to buckling of the flange plate. The reduction of the plate thickness may lead to pinching effects on the hysteretic loops characterizing the cyclic behavior of the fuse. This entails a loss of dissipated energy that could be prevented by reducing the slenderness of the flange plate.

Fig. 20 compares the plastic energy dissipated in conventional frames and in innovative frames with fuse FPM for different peak ground accelerations. In the case of seismic intensity levels equal to PGA = 0.3*g*, the innovative frames dissipate small amounts of plastic energy in fuses, whereas the conventional frames practically remain in the elastic range. For each level of peak ground acceleration, the plastic energy dissipated by fuses in innovative frames is larger than that dissipated by beams in conventional frames. The ground level columns of innovative frames dissipate smaller amounts of hysteretic energy than those of conventional frames for severe seismic excitations (PGA = 0.5*g* and PGA = 0.7*g*). The total amount of dissipated energy is always larger in innovative frames with fuses than in conventional frames.

As well known, the global ductility of the frames significantly depends on the available local ductility. High inelastic deformations and large amounts of plastic energy dissipation require high values of rotation capacity of the plastic hinge regions. Fig. 21 indicates the maximum values of rotations computed in beams and fuses of the first storeys for the different frames under study subjected to severe seismic excitation (PGA = 0.7*g*). As can be noted, the maximum rotations registered in fuses of innovative seismic-resistant frames are larger than those observed in beams of conventional frames. For all the different frames the maximum value of rotation is registered for the fuse A, which exhibits the smallest rotational stiffness; the fuse M presents the smallest maximum rotation among the different fuses. The deformation capacity of the fuses was demonstrated by the results of the experimental tests carried out at Instituto Superior Tècnico of Lisbon, where all specimens showed stable hysteresis loops and were able to achieve rotations equal to 35 mrad. The maximum rotations attained by the fuses of the innovative frames in non-linear dynamic analyses were about 30 mrad, a value for which the fuses of the experimental tests showed good energy dissipation capacity.

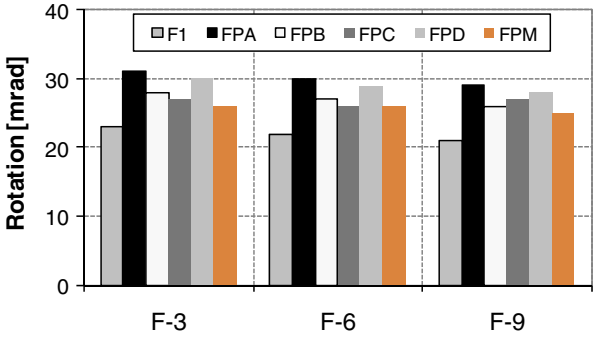

Fig. 21. Maximum rotations in beams (for frames F1) and fuses (for innovative frames FPA, FPB, FPC, FPD, FPM) under PGA = 0.7*g*.

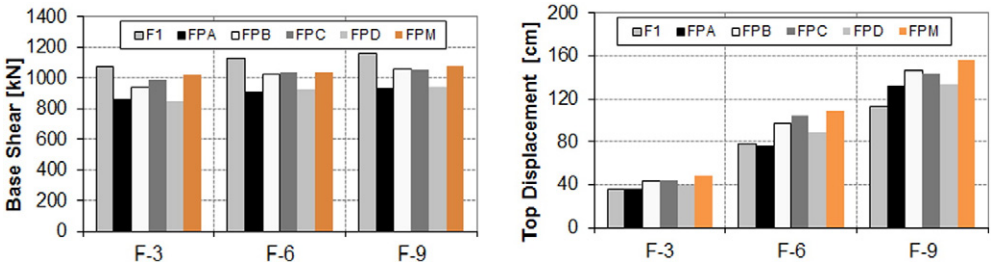

Fig. 22. Base shear and top displacement corresponding to the activation of the plastic mechanism for the different frames from pushover analyses.

5.3. Collapse mechanism assessment

Non-linear static (pushover) analyses were performed in order to study the plastic collapse mechanisms of the different frames. The pushover analyses were conducted under monotonically increasing horizontal loads taking into account both geometric and mechanical non-linearities and confirmed the reduction of the lateral stiffness of the innovative frames with fuses when compared with the conventional frames.

Fig. 22 shows the values of base shear and top displacement corresponding to the activation of the plastic mechanisms for the different frames under study. The values of base shear obtained from pushover analyses are in a good agreement with those obtained from non-linear dynamic analyses for all the structures analyzed. As expected, the innovative seismic-resistant frames with dissipative fuses present lower values of base shear than conventional frames. The decrease of the base shear in the innovative seismic-resistant frames depends on the mechanical characteristics of the fuse devices. A reduction of the bending moment capacity of the fuses causes a decrease of the base shear of the innovative frames.

Moreover, it can be argued that innovative frames with fuses characterized by higher values of the resistance capacity ratio generally provide higher performance levels in terms of ultimate top displacements than conventional frames. Only for the innovative frames FPA-3 and FPA-6 the plastic mechanism is achieved earlier than the conventional frames. In all other cases the top displacements corresponding to the development of the plastic mechanism are much larger for the innovative frames with fuses than for conventional frames. The innovative seismic-resistant frames with fuses characterized by the highest resistance capacity ratios (FPM, FPC and FPB) present the largest values of ultimate top displacements.

The collapse mechanisms obtained from pushover analyses are similar for conventional frames and innovative frames with dissipative fuses. A global collapse mechanism involving the beams and the bases of the ground level columns is registered for both the types of frames. Nevertheless, in conventional frames some plastic hinges are observed in the columns of different storeys. On the contrary, in innovative frames with dissipative fuses plastic hinges are located only in the fuses and at the base of the ground level columns. As well known, it is highly desirable in seismic design to control the location of dissipative zones and the type of post-elastic response in these zones. Global collapse mechanisms with stable and dissipative plastic hinges within all the fuses and at the column bases are preferred due to the high energy dissipation capacity of the frame. It should be observed that an excessive increase of the resistance capacity ratio of fuses close to unity may generate some plastic hinges at the column ends also in innovative frames.

5.4. Effects of different locations of the fuse devices

The efficiency of the fuse devices depends on proper design rules, which include the location of the fuse along with the resistance capacity ratio. The effects of three different locations of the fuse devices on the seismic response of the innovative frames were investigated for the six-storey frames with plates A, C and M. Numerical models of the frames with different distances of the fuse ($L_1 = 25$ cm, $L_2 = 35$ cm, $L_3 = 50$ cm) from the column face were created and analyzed through non-linear dynamic analyses. The results of the numerical analyses confirm that the location of the fuse device is an important design parameter influencing the seismic response of the frames. When the fuse distance measured from the column face increases, the top displacements generally decrease and the base shear enhances, as shown in Fig. 23 and Fig. 24. Moreover, the formation of the first plastic hinges in the devices is deferred and occurs early at the column bases. It can be noted that the variation of the fuse location has smaller effects on top displacements for innovative frames FPM than for other innovative frames.

However, it is necessary to avoid too large distances of the fuses from the column face, since damage would be more easily concentrated in the irreplaceable parts of the frame, such as beams and columns, than in the dissipative devices. Fig. 25 shows a decrease of plastic energy dissipated in fuses and the appearance of damage in beams for the case of fuses with distance equal to $L_3 = 50$ cm.

It is apparent that the location of the fuse should be chosen as a function of the resistance capacity ratio of the device. The results of the analyses show that a satisfactory seismic performance can be achieved selecting a distance of the fuse equal to about the beam depth and values of the resistance capacity ratio within the range of 0.6–0.7.

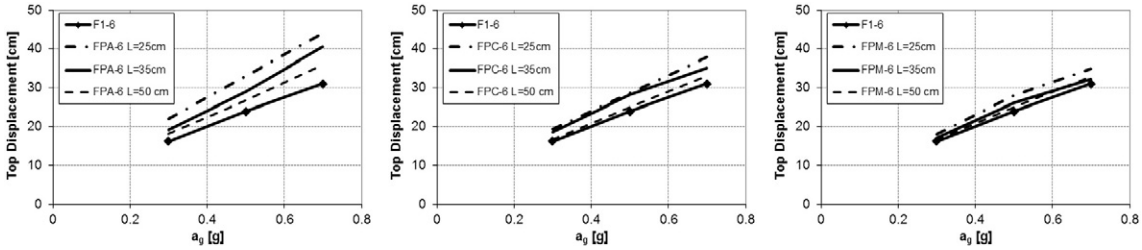

Fig. 23. Maximum top displacement of the six-storey frames (F1, FPA, FPC, FPM) with different locations of fuses for different peak ground accelerations.

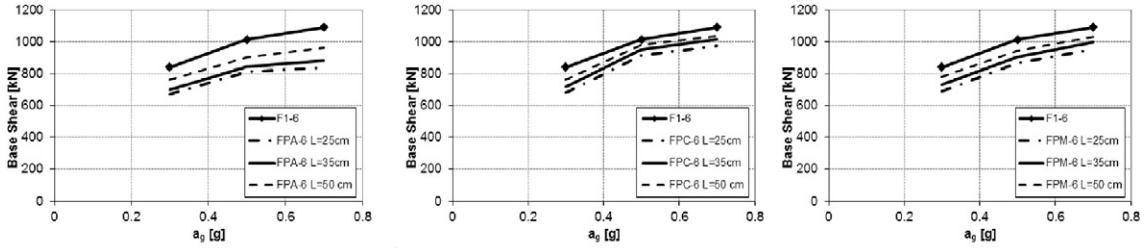

Fig. 24. Maximum base shear of the six-storey frames (F1, FPA, FPC, FPM) with different locations of fuses for different peak ground accelerations.

6. Conclusions

In this paper an innovative fuse device for dissipative beam-to-column connections applicable to multi-storey composite steel buildings has been investigated through numerical simulations. The fuse device consists of steel plates welded to the web and bottom flange of the beam with a specifically detailed slab gap, providing the advantage of replacement in case of damage after severe earthquakes.

- Preliminary numerical investigations carried out by means of detailed finite element models of beam-to-column sub-assemblages show the effectiveness of the fuses. Energy dissipation and plastic deformations concentrate only in the devices, without any significant damage in the other structural elements. The effects of some design parameters on the cyclic response of the fuse devices are evaluated to support the following experimental tests. These preliminary results validate the initial hypothesis for the fuse and confirm that both the steel beam and column remain in the elastic range. The most relevant aspects of the fuse behavior observed in the following experimental tests are conveniently reproduced by the finite element model. The hysteretic behavior of the fuse is mainly affected by buckling of the flange plates under hogging rotation.
- Simple numerical models of the dissipative beam-to-column connections are developed in order to assess the effects of the application of the fuse devices on the seismic response of multi-storey composite steel frames. The properties of the non-linear link elements for the different types of fuse devices are first derived from simple analytical models and then calibrated in order to fit the results of the experimental tests carried out on beam-to-column sub-assemblages.
- The insertion of fuse devices reduces the lateral stiffness of multi-storey composite steel frames. A decrease of the maximum base shear and an increase of the top lateral displacements are observed for the innovative frames with dissipative fuses when compared with the conventional frames in non-linear dynamic analyses. A proper choice of the mechanical characteristics of the fuses may limit the enhancement of the maximum lateral drifts.
- The energy dissipation capacity of the innovative frames is larger than that of the conventional frames. This result can be explained by the higher values of hysteretic energy dissipated by the fuses in innovative frames than by beams in conventional frames. The plastic deformation capacity of the fuses is demonstrated by the results of the experimental tests in which all specimens show stable hysteresis loops and are able to achieve the minimum rotations prescribed by the code. The use of fuse devices in composite steel frames reduces the plastic deformation demand in columns.
- The collapse mechanisms of the innovative frames with fuses are global, ductile and very dissipative, involving all the fuses and the bases of the ground level columns. Plastic deformations and damage concentrate in the fuse devices that are easily replaceable after severe ground motions. The top displacements corresponding to the collapse mechanisms are larger in innovative frames with fuses than in conventional frames.
- The efficiency of the fuse devices depends on the implementation of proper design rules, which include the choice of the resistance capacity ratio and the location of the fuse. The comparison of the seismic performance of the innovative frames with different fuse devices highlights the importance of the resistance capacity ratio. Fuse devices with values of the resistance capacity ratio within a range of 0.6–0.7 generally provide high seismic performance levels in terms of top displacements and ductility, preventing plastic hinge formation in beams and columns. Higher values of the resistance capacity ratio of the fuses entail higher resistant capacities of the frame, but don't guarantee a complete safeguard of the structural elements from damage. Lower values of the resistance capacity ratio of the fuses are more efficient to prevent the spreading of damage in the irreplaceable parts of the frame, but can undermine the seismic performance of the frame mainly in terms of top displacements increase. The distance of the fuse from the column face should be chosen as a function of the resistance capacity ratio of the device. Numerical results show that satisfactory global seismic performance can be achieved selecting a fuse distance equal to about the beam depth and values of the resistance capacity ratio within the range of 0.6–0.7.

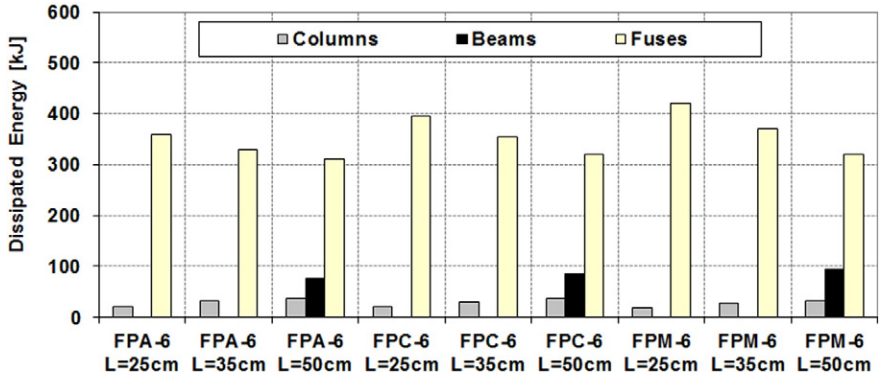

Fig. 25. Plastic energy dissipated in six-storey frames (FPA, FPC, FPM) with different locations of fuses under PGA = 0.7*g*.

Acknowledgments

The studies reported in this paper were conducted within the scope of the FUSEIS (Dissipative Devices for Seismic Resistant Steel Frames, reference RSFR-CT-2008-00032) research project, financed by the Research Fund for Coal and Steel, of the European Commission.

References

[1] A. Plumier, The dogbone: back to the future, Engineering Journal (New York) (1997) 61–67.
[2] L. Calado, J.M. Proenca, M. Espinha, C.A. Castiglioni, Hysteretic behavior of dissipative welded fuses for earthquake resistant composite steel and concrete frames, Steel Compos. Struct. 14 (6) (2013) 547–569.
[3] C.A. Castiglioni, A. Kanyilmaz, L. Calado, Experimental analysis of seismic resistant composite steel frames with dissipative devices, J. Constr. Steel Res. 76 (2012) 1–12.
[4] L. Calado, J.M. Proenca, M. Espinha, C.A. Castiglioni, Hysteretic behavior of dissipative bolted fuses for earthquake resistant steel frames, J. Constr. Steel Res. 85 (2013) 151–162.
[5] D. Danai, G. Dougka, I. Vayas, Seismic behavior of frames with innovative energy dis-sipation systems (FUSEIS1-2), Eng. Struct. 90 (2015) 83–95.
[6] G. Vasdravellis, M. Valente, C.A. Castiglioni, Behavior of exterior partial-strength composite beam-to-column connections: experimental study and numerical simu-lations, J. Constr. Steel Res. 65 (1) (2009) 23–35.
[7] G. Vasdravellis, M. Valente, C.A. Castiglioni, Dynamic response of composite frames with different shear connection degree, J. Constr. Steel Res. 65 (10–11) (2009) 2050–2061.
[8] D. Giannuzzi, R. Ballarini, A. Hucklebridge, M. Pollino, M. Valente, Braced ductile shear panel: new seismic-resistant framing system, Journal of Structural Engineer-ing ASCE 140 (2) (2014) 1–11.
[9] Simulia, ABAQUS Theory Manual, USA, 2014.
[10] I. Mazza, F. Pedrazzoli, Numerical Modeling for Innovative Type of Seismic Moment Resistant Frames with Dissipative, Easy Replaceable, Joints(MSc Thesis) Politecnico di Milano, 2008.
[11] SAP2000 Static and dynamic finite element analysis of structures. Computers and Structures Inc., Berkeley, California.
[12] EN 1998, Eurocode 8: Design of Structures for Earthquake Resistance, 2004.
[13] FEMA 356, Prestandard and Commentary for the Seismic Rehabilitation of Buildings, Federal Emergency Management Agency, Washington DC, USA, 2000.
[14] E.H. Vanmarcke, C.A. Cornell, D.A. Gasparini, S. Hou, SIMQKE: A Program for Artificial Motion Generation, Civil Engineering Department, Massachusetts Institute of Tech-nology, Massachusetts, 1976.
[15] M. Dicleli, A. Mehta, Efficient energy dissipating steel-braced frame to resist seismic loads, Journal of Structural Engineering ASCE 133 (7) (2007) 969–981.